Cell

An Allosteric Mechanism for Activation of the Kinase Domain of Epidermal Growth Factor Receptor

Xuewu Zhang,[1] Jodi Gureasko,[1] Kui Shen,[3,4] Philip A. Cole,[3] and John Kuriyan[1,2,*]
[1] Department of Molecular and Cell Biology and Department of Chemistry and Howard Hughes Medical Institute, University of California, Berkeley, CA 94720, USA
[2] Physical Biosciences Division, Lawrence Berkeley National Laboratory, Berkeley, CA 94720, USA
[3] Department of Pharmacology, Johns Hopkins University School of Medicine, Baltimore, MD 21205, USA
[4] Present Address: Department of Chemistry and Biochemistry, Northern Illinois University, 180 W. Stadium Drive, DeKalb, IL 60115, USA.
*Contact: kuriyan@berkeley.edu
DOI 10.1016/j.cell.2006.05.013

SUMMARY

The mechanism by which the epidermal growth factor receptor (EGFR) is activated upon dimerization has eluded definition. We find that the EGFR kinase domain can be activated by increasing its local concentration or by mutating a leucine (L834R) in the activation loop, the phosphorylation of which is not required for activation. This suggests that the kinase domain is intrinsically autoinhibited, and an intermolecular interaction promotes its activation. Using further mutational analysis and crystallography we demonstrate that the autoinhibited conformation of the EGFR kinase domain resembles that of Src and cyclin-dependent kinases (CDKs). EGFR activation results from the formation of an asymmetric dimer in which the C-terminal lobe of one kinase domain plays a role analogous to that of cyclin in activated CDK/cyclin complexes. The CDK/cyclin-like complex formed by two kinase domains thus explains the activation of EGFR-family receptors by homo- or heterodimerization.

INTRODUCTION

Members of the epidermal growth factor receptor family (EGFR/ErbB1/HER1, ErbB2/HER2, ErbB3/HER3, and ErbB4/HER4) are transmembrane tyrosine kinases that are activated by ligand-induced dimerization (Figure 1A) (Schreiber et al., 1983; Ushiro and Cohen, 1980). These receptors play critical roles in regulating cell proliferation, differentiation, and migration, and their abnormal activation is associated with a variety of human cancers (Yarden and Sliwkowski, 2001).

The structural basis for ligand-induced dimerization of the extracellular region of EGFR family members is now well understood (Cho and Leahy, 2002; Ferguson et al., 2003; Garrett et al., 2002; Ogiso et al., 2002; Schlessinger, 2002). Dimerization results in the phosphorylation of tyrosine residues in the C-terminal tail segments, which serve as docking sites for signaling molecules that contain SH2 or PTB domains and are responsible for onward transmission of the signal (Yarden and Sliwkowski, 2001). EGFR, ErbB2, and ErbB4 contain catalytically competent kinase domains and can form heterodimeric pairs with each other. ErbB3 contains an inactive kinase domain, but it can pair with and activate the other members of the family (Yarden and Sliwkowski, 2001).

The kinase activity of EGFR is stimulated by ligand engagement in a manner that depends on intermolecular interactions (Yarden and Schlessinger, 1987). The purified intracellular region of EGFR is activated by aggregation induced by a variety of agents (Mohammadi et al., 1993; Wedegaertner and Gill, 1989). This activation is not simply due to trans-phosphorylation of the activation loop because, in contrast to most kinases, phosphorylation of the EGFR activation loop is not critical to its activation (Burke and Stern, 1998; Gotoh et al., 1992; Moriki et al., 2001; Stamos et al., 2002).

Crystal structures of the EGFR kinase domain have been determined previously in two distinct crystal lattices. In one (crystal form A) the kinase domain is unphosphorylated but adopts an active conformation, either in a ligand-free form or in complex with the cancer drug Erlotinib (Tarceva) (Stamos et al., 2002). The EGFR kinase domain in a second crystal form (crystal form B; Wood et al., 2004) is bound to the drug Lapatinib (Tykerb) and is in an inactive conformation that resembles closely that of inactive Src-family kinases (Schindler et al., 1999; Xu et al., 1999) and cyclin-dependent kinases (CDKs) (De Bondt et al., 1993).

An activating heterozygous mutation in the activation loop of the kinase domain of EGFR, L834R (also identified as Leu858 in an alternative numbering of the human EGFR

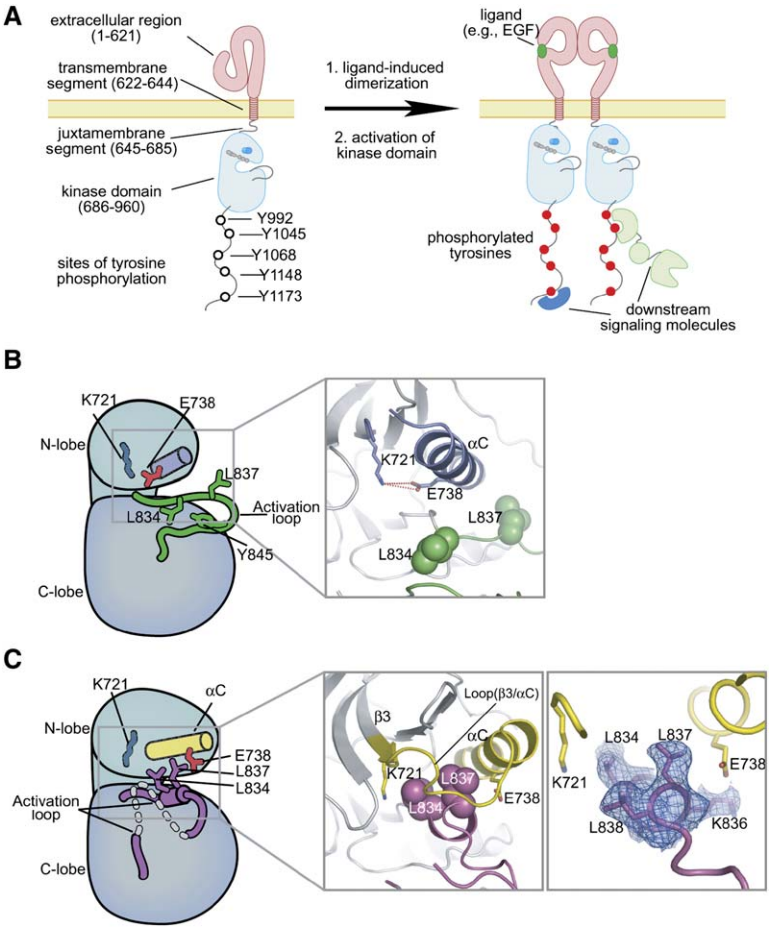

Figure 1. Ligand-Induced Dimerization of EGFR and Active and Inactive States of Its Kinase Domain

(A) General view of the ligand-induced dimerization and activation process of EGFR. The kinase domain is activated through a previously unknown mechanism.

(B) Detailed view of the catalytic site of the EGFR kinase domain in the active conformation. Leu834 and L837 are surface exposed and the Lys721/Glu738 ion pair is intact in this conformation.

(C) Detailed view of the catalytic site in the inactive conformation. Leu834 and L837 pack against helix αC, preventing the formation of the Lys721/Glu738 ion pair. The right panel shows the electron density around residues 834–838 for the V924R kinase domain mutant, at 3σ from a simulated annealing omit map with coefficients $(|F_o| - |F_c|)e^{i\alpha c}$, where the calculated structure factors are generated from a model that does not contain these residues. The structures shown in (B) and (C) were determined in the absence of drug molecules as part of this work and are similar to structures determined previously in complex with the drugs Erlotinib and Lapatinib, respectively (Stamos et al., 2002; Wood et al., 2004).

sequence), has been found frequently in lung cancer patients (accounting for 41% of EGFR mutations in these cancers) (Jiang et al., 2005; Lynch et al., 2004; Paez et al., 2004; Pao et al., 2004; Shigematsu and Gazdar, 2006; Sordella et al., 2004). An adjacent leucine residue (Leu837) is mutated to glutamine in some lung cancer patients (Shigematsu et al., 2005). These residues are either partially (Leu834) or completely (Leu837) surface exposed and do not play an obvious structural role in the active conformation (Figure 1B). In contrast, the importance of these two residues is obvious upon consideration of the Src/CDK-like inactive conformation because both residues pack against hydrophobic sidechains in the interior of the kinase domain while buttressing a displaced orientation of a catalytically critical helix in the N-lobe, helix αC (Figure 1C). Replacement of either leucine by a polar sidechain is likely to destabilize the Src-like inactive conformation and thereby activate the kinase domain. Interestingly, Erlotinib is incompatible with the Src/CDK-like inactive conformation, which may explain why activating mutations potentiate the effectiveness of the closely related drug Gefitinib (Lynch et al., 2004; Paez et al., 2004).

In this paper we show that the isolated kinase domain of EGFR has low basal activity, and that its activity is increased substantially upon replacing Leu834 by arginine. This demonstrates that the wild-type kinase domain on its own is indeed in an autoinhibited state, and we wondered why the original crystal structure of the EGFR kinase domain (Stamos et al., 2002) as well as two new structures we have determined (see below) are in the active conformation. One possibility is that the high protein concentrations used in crystallization (~200 μM) might mimic the high local concentration of kinase domains that is induced by receptor dimerization, leading to the formation of an activated dimer in the crystal lattice. The only available inactive structure of the EGFR kinase domain (crystal form B) is likely to be trapped by the bound kinase inhibitor Lapatinib, which is incompatible with the active structure seen in crystal form A.

Examination of the crystal lattice of the active form of the kinase domain reveals two potentially important crystallographic dimers. One is symmetric, with two kinase domains interacting in a head-to-tail fashion though a primarily electrostatic interface, as discussed before (Landau et al., 2004). The second one is an asymmetric dimer in which one kinase domain interacts with another in a manner analogous to that of a cyclin with an activated cyclin-dependent kinase (Jeffrey et al., 1995). We present

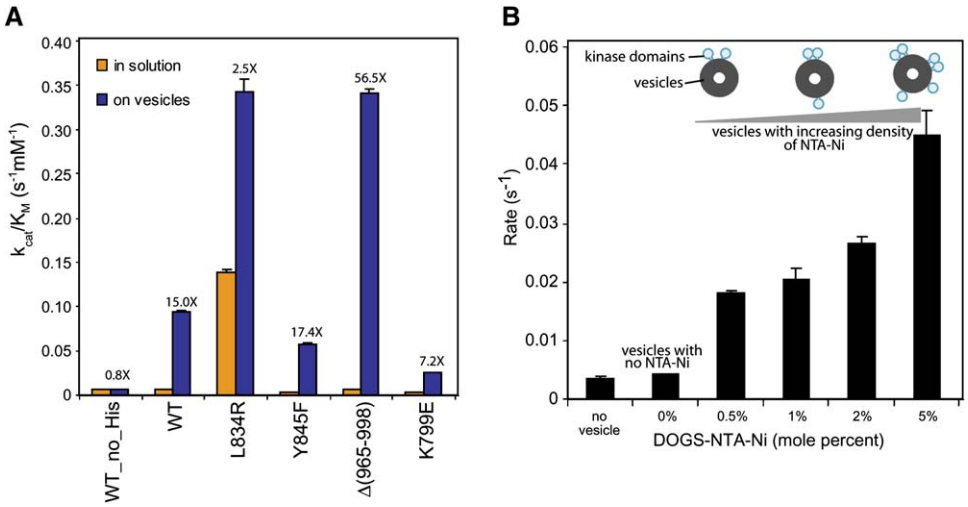

Figure 2. Catalytic Activity of the Wild-Type EGFR Kinase Domain and Various Mutants in Solution and Attached to Lipid Vesicles

(A) Catalytic efficiency (k_{cat}/K_M) of the wild-type and mutants of the EGFR kinase domain in solution (yellow) and linked to vesicles (blue). Fold-increase of the catalytic efficiency upon attachment to vesicles for each protein is indicated on top of the blue bars. WT: wild-type kinase domain (residues 672 to 998). WT_no_His: the wild-type EGFR kinase domain with the $(His)_6$ tag removed. All other proteins in this graph have an intact $(His)_6$ tag. DOGS-NTA-Ni content of vesicles is 5 mole percent in these experiments. Error bars represent standard errors of the linear fittings (see Experimental Procedures). (B) Concentration-dependent activation of the wild-type kinase domain upon attachment to lipid vesicles. The specific activities of the wild-type EGFR kinase domain in solution and with vesicles containing various mole percentages of DOGS-NTA-Ni are shown. The overall concentration of the protein and DOGS-NTA-Ni lipids in the bulk solution are kept fixed at 3.5 μM and 12.5 μM, respectively, for all measurements. Data shown are the means + range of variation from two independent experiments.

a mutational analysis that demonstrates the importance of the CDK/cyclin-like dimer for the activation of the EGFR kinase domain. We also show that the symmetric electrostatic dimer seen in crystal form A (Landau et al., 2004) is unlikely to be relevant for EGFR activation. One compelling aspect of the CDK/cyclin-like model is its ability to explain the interactions of the catalytically dead ErbB3 receptor with other EGFR family members, which we have tested by cotransfecting mammalian cells with active and inactive forms of EGFR. In addition, we have crystallized an EGFR kinase domain variant bearing a mutation (V924R) at the CDK/cyclin-like interface. Strikingly, the mutant EGFR kinase domain crystallizes in a new crystal lattice and adopts an inactive Src/CDK-like conformation.

RESULTS AND DISCUSSION

The EGFR Kinase Domain Is Autoinhibited and Can Be Activated in a Concentration-Dependent Manner when Localized to Vesicle Surfaces

We expressed and purified the L834R mutant form of the kinase domain (residues 672–998 with an N-terminal His-tag) and measured its kinase activity toward a peptide substrate. The value of the catalytic efficiency (k_{cat}/K_M) for the L834R mutant is ~20-fold higher than that for the wild-type kinase domain, indicating that the wild-type kinase domain is autoinhibited (Figure 2A).

The EGFR kinase domain is monomeric in solution at concentrations up to 50 μM (Figure S1). The local concentration of kinase domains in a dimeric receptor is estimated to be in the millimolar range. In order to increase the local concentration in a controlled fashion we added a hexa-histidine tag to the kinase domain and localized it to the surface of small unilamellar vesicles containing lipids with a nickel-nitrilotriacetate head group (1, 2-Dioleoyl-*sn*-Glycero-3-{[N(5-Amino-1-Carboxypentyl)iminodi-Acetic Acid]Succinyl} Nickel salt, DOGS-NTA-Ni) (Dorn et al., 1998). The density of the kinase domain on individual vesicles was controlled by varying the mole ratio of the DOGS-NTA-Ni lipids and the 1,2-Dioleoyl-*sn*-Glycero-3-Phosphocholine (DOPC) lipids that constitute the vesicles. A similar method has been used to study the activation of the CheA histidine kinase by the aspartate receptor from *E. coli* (Shrout et al., 2003).

The density of DOGS-NTA-Ni lipids in the vesicles is varied from 0.5 to 5.0 mole percent. The dissociation constant for attachment of the His-tagged kinase domain to the vesicle is estimated to be ~2 μM and the total concentration of DOGS-NTA-Ni lipid is maintained at 12.5 μM in these experiments to ensure localization of the His-tagged protein to the vesicles. The effective local concentration of kinase domains is approximately in the range of ~0.4 mM (for 100 nm vesicles containing 0.5 mole % DOGS-NTA-Ni) to ~4 mM (for 5 mole % DOGS-NTA-Ni) (see Table S1).

The wild-type kinase domain attached to vesicles displays a significantly increased catalytic activity relative to that of the kinase domain in solution (up to ~15-fold increase in the value of k_{cat}/K_M) (Figure 2). The specific activity increases when the density of the kinase molecules on individual vesicles is increased, while keeping the

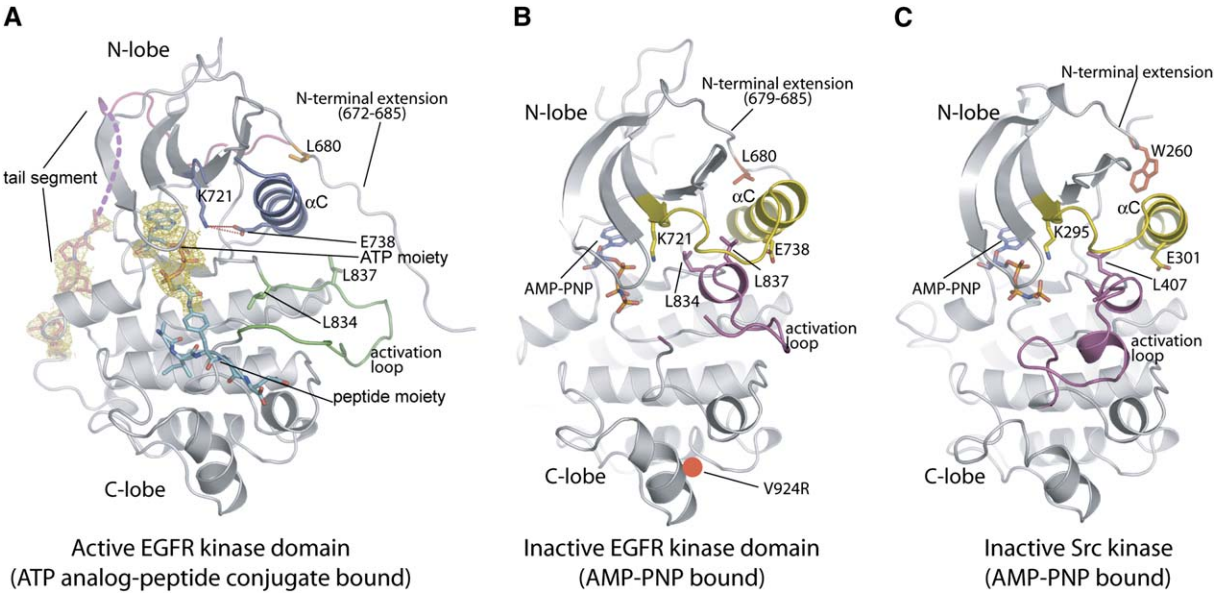

Figure 3. Crystal Structures of the EGFR Kinase Domain in the Active and Inactive Conformations

(A) Crystal structure of the EGFR kinase domain in complex with the ATP analog substrate peptide conjugate. The kinase adopts an active conformation. Electron density (calculated in the same way as in Figure 1C) for the ATP moiety of the ATP analog-peptide conjugate and seven residues in the C-terminal tail segment is shown in yellow.

(B) Crystal structure of the V924R mutant of the EGFR kinase domain in complex with AMP-PNP. The kinase adopts a Src/CDK-like inactive conformation. The approximate location of the V924R mutation is indicated.

(C) Crystal structure of an inactive Src kinase in complex with AMP-PNP (PDB ID: 2SRC).

overall concentrations of the His-tagged kinase domain and DOGS-NTA-Ni constant (Figure 2B). This suggests that an intermolecular interaction is involved in the activation of the kinase domain.

Vesicles containing no DOGS-NTA-Ni lipids do not stimulate the level of kinase activity (Figure 2B). Conversely, removal of the His-tag by proteolytic cleavage does not result in an increase in catalytic activity in the presence of the DOGS-NTA-Ni-containing vesicles; the basal activity in solution is unchanged by the proteolytic treatment (Figure 2A). These experiments rule out the possibility that the activation of the vesicle-linked kinase domain is due to nonspecific interactions between the lipids and the protein.

One simple explanation for the concentration dependence of the activation of the vesicle-linked kinase domain is that it is a consequence of increased trans-phosphorylation of the kinase domain on Tyr845 in the activation loop, which corresponds to the site of activating phosphorylation in many kinases (Huse and Kuriyan, 2002). This is ruled out by experiments on a mutant form of the EGFR kinase domain with this tyrosine residue replaced by phenylalanine (Y845F). Y845F is activated upon attachment to vesicles to a similar extent as the wild-type EGFR kinase domain (Figure 2A).

New Crystal Structures of the EGFR Kinase Domain in an Active Conformation

We screened extensively for conditions that yield crystals of the wild-type EGFR kinase domain but succeeded only in obtaining crystals with the same lattice as described previously (Stamos et al., 2002), although under very different conditions. We obtained crystals of the apo-EGFR kinase domain in 25% PEG4K, 6% isopropanol, 100 mM HEPES, pH 7.5. Two different ATP analog-peptide conjugates were used for crystallization with the EGFR kinase domain. In one the peptide segment corresponds to 12 residues spanning Tyr1173 in the C-terminal tail of EGFR, but cocrystallization trials yielded crystals in 1 M NaMalonate, 100 mM HEPES, pH 7.0 that do not appear to contain the substrate analog. Crystals of the kinase domain in complex with another ATP analog-peptide conjugate (corresponding to a c-Src substrate; Levinson et al., 2006) were grown in 18% PEG3350, 0.2 M LiCitrate, 100 mM HEPES, pH 7.5. The unit cell parameters for these crystals are very similar to those for the original form A crystals, which were obtained under different conditions (1 M Na/K tartrate, 100 mM MES, pH 7.0) (Stamos et al., 2002).

The structure of the kinase domain complexed with the ATP analog-peptide conjugate (Figures 1B and 3A) shows that all the catalytic residues are positioned appropriately for catalysis, as judged by comparison with the structures of insulin receptor kinase-substrate complexes (Parang et al., 2001). Given the persistent formation of crystal form A under a wide variety of crystallization conditions, we wondered whether an intrinsic tendency of the kinase domain to dimerize at high concentrations may promote the formation of a specific crystal lattice that stabilizes

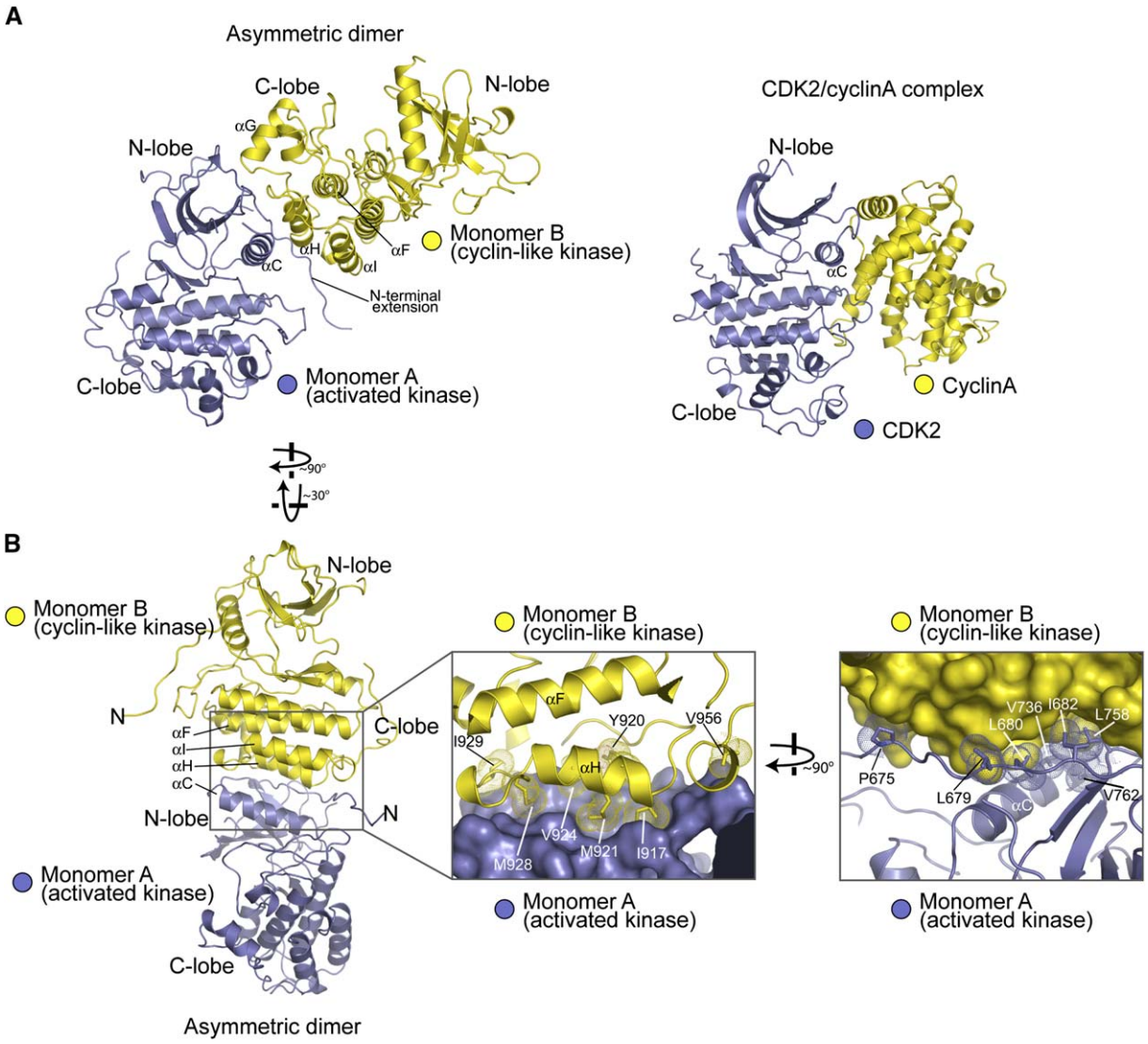

Figure 4. The Asymmetric CDK/Cyclin-like Crystallographic Dimer of the EGFR Kinase Domain

(A) Overview of the asymmetric dimer, and comparison with the structure of the CDK2/cyclinA complex (PDB ID: 1HCL).

(B) Detailed view of the asymmetric dimer interface. Monomer A (the activated kinase) is shown in surface representation in the first exploded view. Hydrophobic interfacial residues from monomer B are highlighted. In the second exploded view monomer B (the cyclin-like kinase) is shown in surface representation, and hydrophobic interfacial residues from monomer A are highlighted.

the active conformation. Previous analysis of crystal form A had focused attention on a symmetric crystallographic dimer held together primarily by electrostatic interactions (Landau et al., 2004). Crystal form A also contains an extensive hydrophobic interface between two kinase domains that results from a 3-fold screw rotation (Figures 4A and 4B) (i.e., one kinase domain in a pair is rotated by 120° about an axis relative to the other one and is also translated along that axis by 42 Å; see Figure S3A for the precise transformation). This asymmetric dimer juxtaposes the C-lobe of one kinase domain (monomer B) against the N-lobe (with extensive interactions spanning helix αC) of the other kinase domain (monomer A) (Figures 4A and 4B).

A striking aspect of the asymmetric interaction between the two EGFR kinase domains in the second dimer is its resemblance to the interaction between activated CDK2 and cyclinA (Figure 4A), with the C-lobe of monomer B in the EGFR kinase dimer taking a position relative to monomer A that is analogous to that of cyclinA in the active CDK/cyclin complex (Jeffrey et al., 1995). Although the structure of the C-lobe of the kinase domain is unrelated to that of the cyclins, key elements of the interaction, particularly the engagement of helix αC of monomer A, are

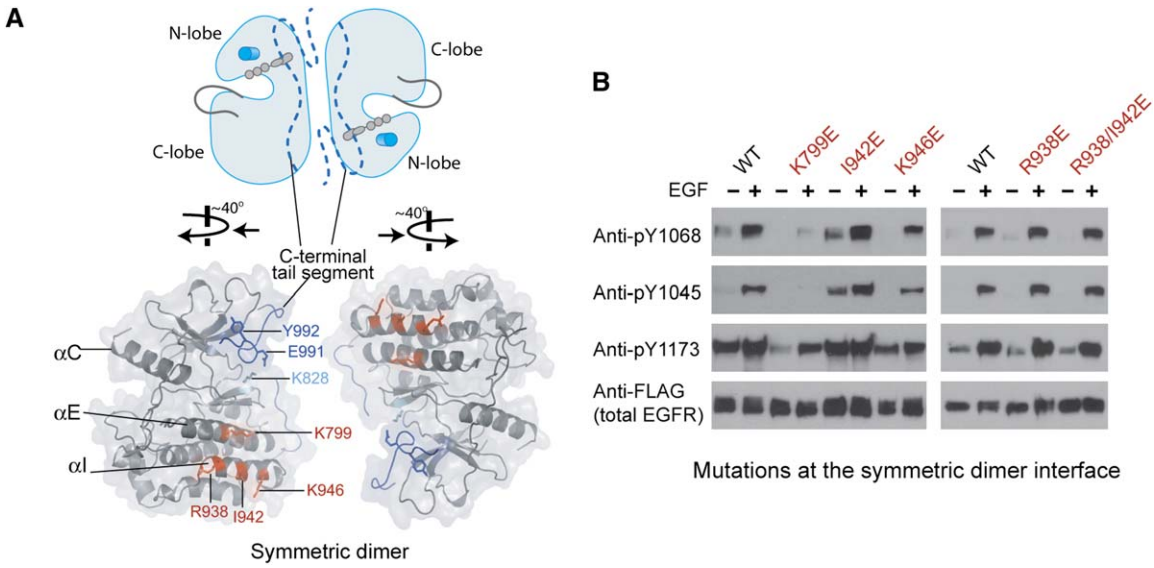

Figure 5. The Symmetric Electrostatic Dimer Is Not Important for EGFR Activation

(A) Residues involved in the symmetric dimer interface. The two monomers are moved away and rotated relative to each other as indicated to provide a clearer view of residues involved in the dimer interface. Blue: residues in the C-terminal tail segment (Glu991 and Tyr992); Cyan: residue in the N-lobe of the kinase (Lys828); Red: residues in the C-lobe of the kinase (Lys799, Arg938, Ile942, and Lys946).

(B) Mutations of interfacial residues in the C-lobe of the kinases, except K799E, do not affect receptor phosphorylation. The anomalous behavior of K799E is not understood (see Supplemental Data).

similar in general terms. An insightful earlier study had proposed several potential models for dimerization of the EGFR kinase domain in the absence of direct structural information and had speculated that the base of the C-lobe of the kinase domain might engage helix αC of another kinase domain through hydrophobic interactions (Groenen et al., 1997).

The Symmetric Dimer Seen in the Crystals of the Active Kinase Domain Does Not Play a Significant Role in the Activation of EGFR

We have measured the effect on EGFR activation of mutations at the symmetric dimer interface (Figure 5A) by using a cell transfection assay in which the levels of phosphorylation at three sites in the C-terminal tail of the full-length receptor (Tyr1045, Tyr1068, and Tyr1173) are monitored. Four of these mutant receptors (I942E, K946E, R938E, and a double mutant R938/I942E) show a robust response to EGF stimulation (Figure 5B). Given the central location of these residues within the symmetric dimer interface, these results argue against the importance of this dimer in the activation process (see Supplemental Data for more information).

Further evidence that the symmetric dimer is not involved in the activation process is provided by the vesicle-linked assay for the activity of the kinase domain. The C-terminal tail segment is a central element of the symmetric dimer, but a variant of the kinase domain in which the majority of the C-terminal tail segment is removed (containing a deletion spanning residues 965–998) is activated upon attachment to vesicles to a much higher level than seen for the kinase domain with the intact C-terminal fragment (Figure 2A). These results indicate that the C-terminal tail segment suppresses the catalytic activity of EGFR kinase domain, consistent with previous studies (Chang et al., 1995; Wood et al., 2004), but is not required for the activation mechanism.

An Allosteric Activation Mechanism Suggested by the Asymmetric EGFR Kinase Domain Dimer

The CDK/cyclin-like dimer interface is formed by the N-terminal extension (residues 672–685), the C helix, and the loop between strands β4 and β5 of monomer A (the activated kinase domain) and the loop between helices αG and αH, helix αH, and the end of helix αI from monomer B (the cyclin-like kinase domain), burying ~2019 Å^2 of surface area between them (Figure 4). As in the CDK2/cyclinA interface (Jeffrey et al., 1995), the core of the asymmetric EGFR kinase domain dimer is dominated by hydrophobic interactions, involving primarily residues Leu680, Ile682, Leu736, Leu758, and Val762 from monomer A (in the N-lobe of the activated kinase) and Ile917, Tyr920, Met921, Val924, and Met928 from monomer B (in the C-lobe of the cyclin-like molecule) (Figure 4B). Several hydrogen bonds are also present at the periphery of the interface.

Many features of the Src/CDK-like inactive conformation are incompatible with formation of the CDK/cyclin-like interface. For example, the N-terminal extension adopts an extended conformation in the active structure and forms part of the CDK/cyclin-like dimer interface (Figure 4B). This forces the removal of the side chain of Leu680 out of a hydrophobic pocket that is formed between helix αC and strand β5 in the inactive structure (Wood et al., 2004) and into the heart of the CDK/cyclin-like interface (Figure 4B). The residue corresponding to Leu680 in c-Src, Hck, and Abl is a tryptophan residue

(Trp260 in c-Src) that acts as a wedge between helix αC and the main body of the kinase domain in the Src/CDK-like inactive conformation, preventing activation (Levinson et al., 2006; Xu et al., 1999).

The 3-fold screw axis that generates the asymmetric CDK/cyclin-like dimer positions the two kinase domains such that their N-terminal residues are ~50 Å apart and can both be connected, in principle, to the juxtamembrane and transmembrane segments presented at the membrane surface (Figure 4). The precise disposition of the C-terminal ends of the extracellular domains in an activated EGFR dimer is unknown, but they are estimated to be ~20 Å apart (Burgess et al., 2003). This gap between the ends of the dimeric extracellular region and the asymmetric CDK/cyclin-like dimer could be compensated for by residues 615–671 of the receptors, which are between the two regions and are not present in the crystal structures. If the juxtamembrane segment retains a degree of flexibility, then it is possible that the two kinase domains in the dimer can switch positions dynamically and activate each other. The juxtamembrane and transmembrane segments may have other important regulatory roles (McLaughlin et al., 2005) and may prevent activation of the kinase domain when ligand-independent dimers are formed (Moriki et al., 2001).

The generation of an open-ended higher-order oligomer of kinase domains along the 3-fold screw axis appears unlikely within the context of the full-length receptor at the cellular membrane because a third kinase domain would have its N-terminal segment pointing away from the plane of the membrane (Figure S3A). We conclude therefore that activation of EGFR involves the formation of a CDK/cyclin-like dimer of kinase domains, as illustrated in Figure 4.

A sequence alignment of EGFR family members shows that the residues involved in the N- or the C-lobe faces of the CDK/cyclin-like interaction are essentially invariant in the three catalytically active EGFR family members (EGFR, HER2, and HER4) (Figure 7A), strongly suggesting that HER2 and HER4 are autoinhibited and activated by the same mechanism (Figure 7B). The sequence comparisons show that residues in ErbB3 that correspond to the C-lobe face of the interface (i.e., the cyclin-like face) are very similar to the residues found in other members in the family. In contrast, residues in ErbB3 that correspond to the N-lobe face (i.e., on the kinase domain that is being activated) are divergent (Figure 7A). This suggests that the catalytically inactive ErbB3 molecule functions essentially as a cyclin-like activator for other EGFR family members. ErbB3 itself does not need to be activated, and we presume that there has been no selective pressure for maintaining residues at the N-lobe face of ErbB3.

Crystal Structure of the V924R Mutant of the EGFR Kinase Domain Reveals a Src/CDK-like Inactive Conformation

The Src/CDK-like inactive conformation of the EGFR kinase domain has only been observed in a complex with the drug Lapatinib (Wood et al., 2004), leaving open the possibility that this particular conformation is induced by the drug. We introduced a mutation (V924R) in the EGFR kinase domain, located in the center of the C-lobe face of the CDK/cyclin-like dimer interface, and crystallized the mutant protein in the presence of the ATP analog AMP-PNP and determined its structure at 2.6 Å resolution (Table S3).

The mutant EGFR kinase domain crystallizes in a new crystal form, with two molecules in the asymmetric unit. The structures of the two monomers are essentially identical and are very similar to that of the previously determined Lapatinib complex (Figure S4B). Strong electron density is present for the N-terminal base of the activation loop, which forms a helical turn, stabilizing the outwardly displaced helix αC (Figures 1C and 3B). Our structure also permits visualization of the loop leading into helix αC (Figures 1C and 3B), which is disordered in the Lapatinib complex. This loop makes close interactions with the inactive helical conformation of the N-terminal base of the activation loop, explaining the activating effect of another set of lung cancer mutations in EGFR, in which this loop is deleted (Lynch et al., 2004; Paez et al., 2004; Shigematsu and Gazdar, 2006; Sordella et al., 2004).

Our ability to generate crystals of the EGFR kinase domain in an inactive Src/CDK-like conformation by introducing a single mutation in the C-lobe of the kinase, located far from the active site, provides strong support for the concept that the active conformation previously seen in crystals of the EGFR kinase domain is a consequence of mimicry by the crystal of an intrinsic activation mechanism that moves the kinase domain away from the otherwise stable inactive Src/Cdk-like conformation.

Mutations in Full-Length EGFR Show that the CDK/Cyclin-like Asymmetric Dimer Interface Is Required for Activation of the Receptor

We mutated several residues that are located at the CDK/cyclin-like dimer interface and tested the effects of these mutations on autophosphorylation of full-length EGFR in the cell-based assay. These mutations include P675G, L680A, L680N, I682Q, and L736R, which involve residues contributed to the interface by monomer A (the activated kinase), and I917R, M921R, V924R, and M928R, involving residues that are contributed to the interface by monomer B (the cyclin-like partner). All of these mutations, except L680A, almost completely abrogate the ability of EGFR to phosphorylate all three of the tested autophosphorylation sites, either before or after EGF stimulation (Figure 6A). L680A displays modestly decreased levels of phosphorylation compared to the wild-type EGFR. Replacement of Leu680 by alanine removes the inhibitory wedge between helix αC and β5, which is expected to activate the kinase. On the other hand, the mutation is also predicted to destabilize the asymmetric dimer interface in the active complex. The observed result for this mutation is likely to be a combination of these two effects. Replacement of Leu680 by asparagine completely shuts down the kinase

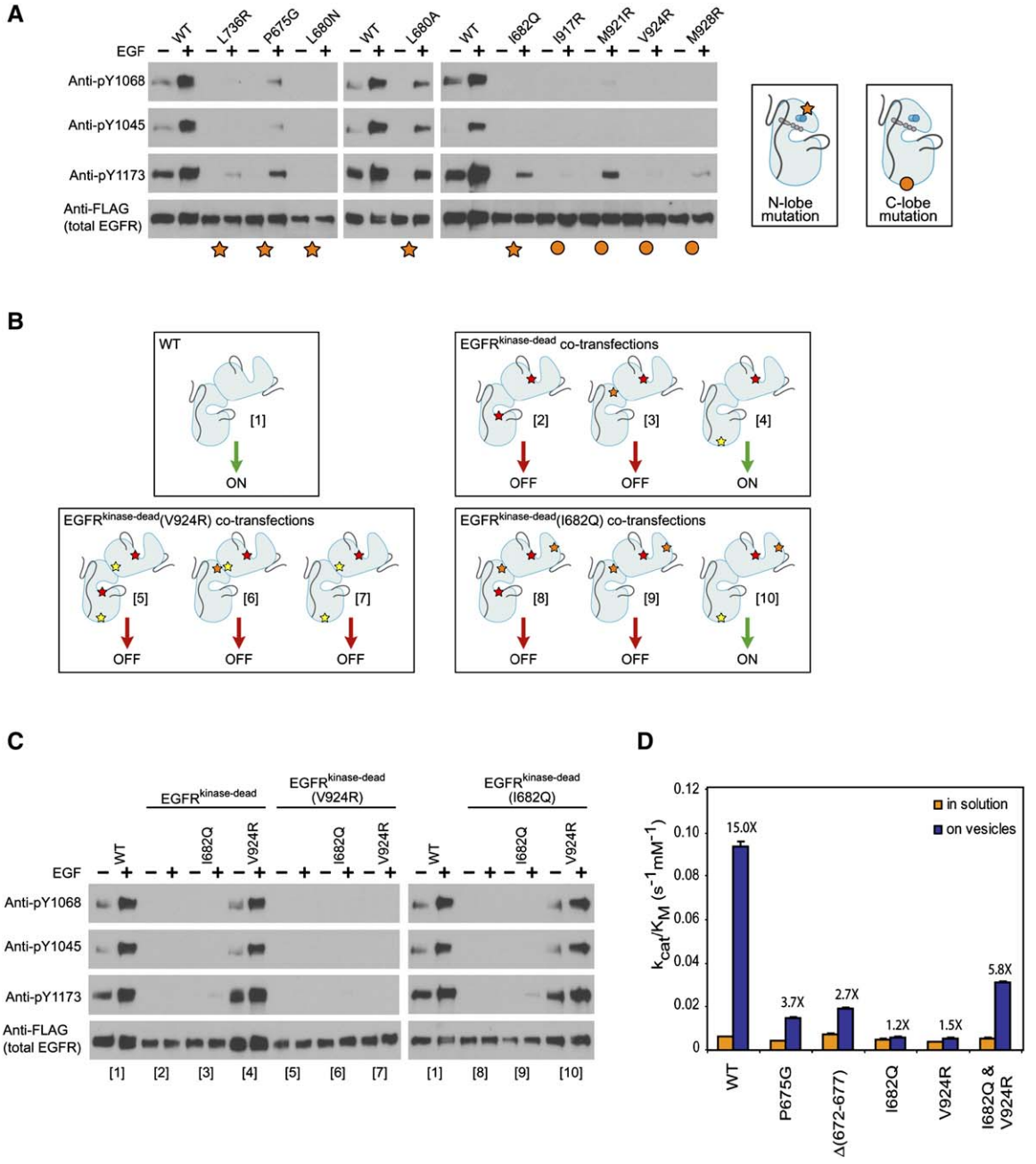

Figure 6. The Asymmetric Dimer Interface Is Important for EGFR Activation

(A) Single mutations at the asymmetric dimer interface abolish EGFR phosphorylation. Stars and circles denote mutations in the N-lobe and C-lobe face of the dimer interface, respectively.

(B) Predicted outcomes of a variety of transfection/cotransfection experiments based on the model. Red, orange, and yellow stars denote mutations in the catalytic site, N-lobe face, and C-lobe face of the dimer interface, respectively. Different combinations are numbered 1 through 10.

(C) Results of the transfection/cotransfection experiments. Combination numbers under the transfection experiments correspond to those in (B).

(D) Effect of mutations in the asymmetric dimer interface on the catalytic activity of the kinase domain in solution and attached to lipid vesicles. DOGS-NTA-Ni content of vesicles is 5 mole percent. Fold-increase of the catalytic activity upon attachment to vesicles for each protein is indicated on top of the blue bars. Error bars represent standard error of the linear fitting (see Experimental Procedures).

(Figure 6A), presumably because asparagine is less well accommodated at the hydrophobic CDK/cyclin-like interface than alanine.

In order to further test the model and also rule out that the observed lack of activation of mutant receptors is due to misfolding or other problems, we determined the

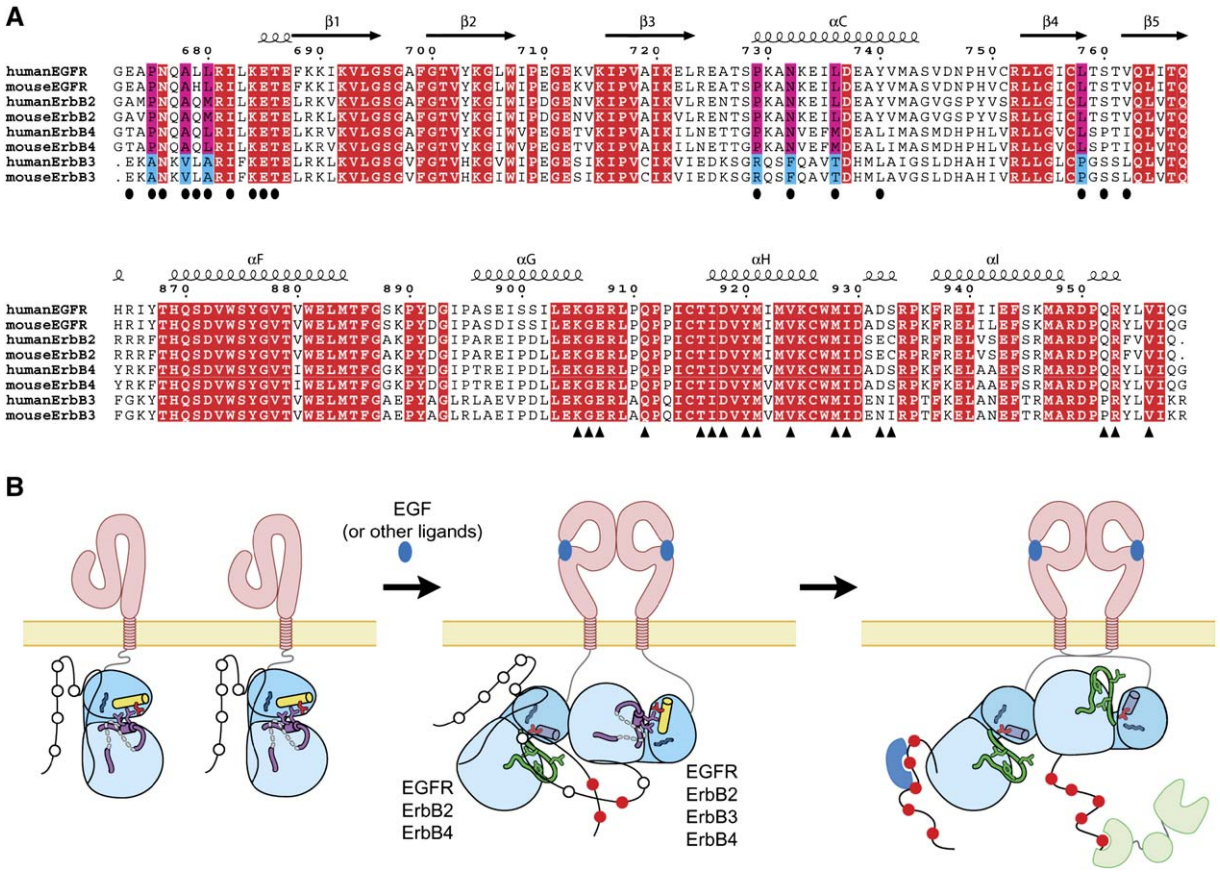

Figure 7. A General Model for the Activation of Members of the EGFR Family

(A) Sequence alignment of the EGFR family members from human and mouse. Two regions containing residues involved in the N- and C-lobe faces of the dimer interface are shown in the upper and lower panels, respectively. Identical residues are colored in red. Residues in the N- and C-lobe faces of the dimer interface are denoted by ovals and triangles, respectively. Magenta and cyan highlight residues in the dimer interface that are conserved among EGFR, ErbB2, and ErbB4 but not in ErbB3.

(B) A general model of the activation mechanism for the EGFR family receptor tyrosine kinases. All the members in the family can act as the cyclin-like activator for the kinase-active members (EGFR, ErbB2, and ErbB4) after ligand-induced homo- or heterodimerization.

ability of one mutant to activate the other in trans. Since the dimer interface is asymmetric, the model predicts that an EGFR molecule with a mutation in the C-lobe face of the dimer interface (i.e., with the cyclin-like face disrupted) can be activated by another EGFR molecule that has an intact C-lobe interface. Conversely, an EGFR molecule with a mutation in the N-lobe face of the dimer interface (i.e., one that is predicted to be resistant to activation) can act as a cyclin-like activator for another EGFR molecule in which the N-lobe face is intact. In order to test these predictions we constructed a catalytically dead variant of EGFR in which Asp813 (the catalytic base in the kinase domain) is replaced by asparagine (EGFR$^{kinase\text{-}dead}$). Transfection of cells with EGFR$^{kinase\text{-}dead}$ shows that it does not undergo autophosphorylation either before or after EGF stimulation (Figure 6C).

Cotransfection of EGFR$^{kinase\text{-}dead}$ with EGFR(I682Q) (an N-lobe mutant) does not result in detectable levels of autophosphorylation (Figure 6C, combination [3]). In contrast, cotransfection of EGFR$^{kinase\text{-}dead}$ with EGFR(V924R) results in robust levels of autophosphorylation (Figure 6C, combination [4]). In this case the catalytically active EGFR(V924R) (a C-lobe mutant) has an intact N-lobe face, and although it cannot stimulate itself because of its disrupted C-lobe face, it can be stimulated by the intact C-lobe of EGFR$^{kinase\text{-}dead}$ (Figure 6B, combination [4]). We also generated a double mutant, EGFR$^{kinase\text{-}dead}$(I682Q), which rescues the autophosphorylation of EGFR(V924R) because it has an intact C-lobe that can interact with the intact N-lobe of EGFR(V924R) (Figures 6B and 6C, combination [10]).

Also consistent with the model is the inability of EGFR$^{kinase\text{-}dead}$(I682Q) to rescue autophosphorylation of EGFR(I682Q) (Figure 6C, combination [9]). In this case, both transfected EGFR molecules have defective N-lobe faces (Figures 6B and 6C, combination [9]). Likewise, a double mutant EGFR$^{kinase\text{-}dead}$(V924R) (defective C-lobe face) failed to rescue the autophosphorylation of

either EGFR(I682Q) or EGFR(V924R) (Figures 6B and 6C, combination [6] and [7]). Additional experiments, including mutation of Tyr845 in the activation loop, are presented in Supplemental Data.

The CDK/Cyclin-like Interface Is Required for the Concentration-Dependent Activation of the EGFR Kinase Domain

Pro675 is within the extended N-terminal extension of the kinase domain and makes a hydrophobic contact with Val956 at the asymmetric dimer interface (Figure 4B). A kinase domain variant containing a P675G mutation possesses basal kinase activity comparable to that of the wild-type kinase domain in solution and is only activated ~3- to 4-fold when localized to vesicles (Figure 6D). Another variant of the kinase domain with a deletion around Pro675 (Δ672–677) also shows similar behavior, with roughly wild-type levels of basal activity but only ~3-fold stimulation upon binding to vesicles.

We also tested two variants of the EGFR kinase domain that contain the I682Q and V924R mutations in the vesicle-linked assay. These two mutant kinase domains show basal levels of activity comparable to that of the wild-type (Figure 6D). Upon linking to vesicles, I682Q and V924R show virtually no increase in their catalytic activities (1.2- and 1.5-fold increase for I682Q and V924R, respectively) (Figure 6D).

We determined the catalytic activity of an equimolar mixture of these two mutant forms of the EGFR kinase domain in the absence and presence of lipid vesicles. The results show that the basal activity of this mixture of the two mutants is very similar to that of the individual mutants and to that of the wild-type kinase domain. The activity is stimulated ~6-fold when the proteins are linked to vesicles (Figure 6D), suggesting that V924R (defective C-lobe) is activated by I682Q (defective N-lobe) through heterodimerization on the surface of vesicles. In this case only half of the kinase molecules (i.e., V924R) can be activated, which explains why the level of stimulation is not as high as that seen for the wild-type kinase upon attachment to vesicles.

It has been shown that a mutant of EGFR with a truncated intracellular region exerts a dominant-negative effect on cotransfected wild-type EGFR (Kashles et al., 1991), which suggests that dimerization of the intracellular region is required for the activation of EGFR. More evidence supporting our model includes a study showing that a catalytically dead mutant of EGFR (K721M) heterodimerizes with and activates ErbB2, which lacks a physiological ligand, in an EGF-dependent manner (Deb et al., 2001).

Conclusions

The model presented here, in which one EGFR kinase domain in a dimer acts as a cyclin-like activator for the other, provides a precise molecular basis for the autoinhibition and EGF-induced acquisition of catalytic activity by EGFR. The elegant and simple model for EGFR activation proposed by Schlessinger (reviewed in Schlessinger, 2002) contains as its central feature the direct communication of the arrival of an external signal to the interior of the cell by the conversion of a monomeric receptor to a ligand-induced dimer. The activation of EGFR has such serious consequences for the cell that nature has clearly evolved secondary levels of control that minimize inappropriate activation of the receptor through intermolecular collisions. The dimerization interface of the extracellular domains is kept hidden until unmasked by EGF (Burgess et al., 2003). In this paper we show that the kinase domain of EGFR is itself responsive to the dimerization of the receptors, converting from an inactive Src/CDK-like conformation to an active one in response to an increase in the local concentration of the receptor. The fundamental on/off switch utilized by EGFR at the level of the kinase domain is the same as that used by the CDK/cyclin complexes, except that EGFR and its relatives serve as their own "cyclins."

The acquisition of allosteric mechanisms in protein systems appears to evolve opportunistically, with a fundamental function modulated in different ways as a consequence of random mutation and selection. In the case of receptor tyrosine kinases it is the monomer-dimer equilibrium that is likely to be fundamental (Schlessinger, 2002), with the cyclin-like activation of EGFR being a specialized variation that may not be utilized by other receptors. Within the EGFR family, however, the pairwise ability of the kinase domains to act as activators as well as transducers for each other clearly leads to a powerful combinatorial response to a diversity of ligands.

EXPERIMENTAL PROCEDURES

Expression and Purification of the Kinase Domain

DNA encoding residues 672–998 of human EGFR was cloned into pFAST BAC HT (Invitrogen) using the NcoI and HindIII restriction sites. The construct contains an N-terminal 6-His tag, a linker, and a cleavage site for the Tobacco Etch Virus protease(TEV) (MSYYHHHHHHDY DIPTTENLYFQGAM). All mutations were introduced using the Quikchange site-directed mutagenesis kit (Stratagene). Sequences of all the plasmids were confirmed by DNA sequencing.

Recombinant bacmid (Bac-to-Bac expression system, Gibco BRL) were transfected into Sf9 cells to produce recombinant baculovirus, which were used to infect Sf9 cells grown in suspension. Cells were harvested 2–3 days after infection by centrifugation at 4000 × g and resuspended in a buffer containing 50 mM Tris, 5% glycerol, 1 mM DTT, and protease inhibitor cocktail (Roche), pH 8.0. Cells were homogenized by french press in resuspension buffer and the lysate was centrifuged at 40000 × g for 45 min. The supernatant was loaded onto a 60 ml Q-Sepharose Fastflow column (Amersham) equilibrated in buffer A (50 mM Tris, 5% glycerol, and 15 mM β-mercaptolethanol, pH 8.0). Proteins were eluted using buffer A plus 1 M NaCl and loaded onto a 1 ml Histrap column (Amersham) pre-equilibrated with buffer B (20 mM Tris, 500 mM NaCl, 5% glycerol, 20 mM imidazole, pH 8.0). Proteins were eluted using a gradient of imidazole (20–250 mM) after extensive wash with buffer B. The proteins were either purified immediately using a 6 ml Uno-Q column (Bio-rad) to produce His-tagged kinase domains, or treated with the TEV protease overnight at 4°C to remove the N-terminal His-tag before being subjected to Uno-Q purification for crystallization, analytical ultracentrifugation, and static light scattering.

Proteins were diluted 10-fold using buffer C (20 mM Tris, 20 mM NaCl, 5% Glycerol, and 2 mM DTT, pH 8.0) and loaded onto the

Uno-Q column pre-equilibrated with buffer C. Proteins were eluted using a gradient of NaCl (20–500 mM). Fractions containing the EGFR protein were pooled, concentrated, and buffer exchanged into 20 mM Tris, 50 mM NaCl, 2 mM DTT, and 2 mM TCEP, pH 8.0. Proteins were concentrated to 10–30 mg/ml and flash-frozen in liquid nitrogen and stored at −80°C. Mass spectrometric analysis was used to confirm the identity of the proteins (mass spectrum of the Y845F mutant is shown in Figure S6).

Preparation of Small Unilamellar Vesicles

DOPC and DOGS-NTA-Ni lipids in chloroform (Avanti Polar Lipids, Inc) were mixed in a glass tube. A lipid film was formed upon removing chloroform under a stream of argon gas, followed by putting the tube under vacuum for at least 3 hr. Rehydration buffer (10 mM $MgCl_2$, 20 mM Tris, pH 7.5) was added to the lipid film and incubated for at least 3 hr. Intermittent vigorous vortexing during the incubation was applied to convert the lipid film into large, multilamellar vesicles. These mutilamellar vesicles were then forced through a polycarbonate filter (pore size: 100 nm) 21–41 times using a mini-extruder (Avanti Polar Lipids, Inc) to yield homogenous small unilamellar vesicles. The diameter of the vesicles was measured to range from 100–200 nm by static light scattering (Figure S2).

Kinase Assay in Solution and with Vesicles

A continuous enzyme-coupled kinase assay was performed to measure the kinase activity of the proteins as described (Barker et al., 1995), with minor modifications. The ATP concentration was kept at 0.5 mM in all the assays. The buffer used contains 10 mM $MgCl_2$, 20 mM Tris, pH 7.5 (replacement of $MgCl_2$ by $MnCl_2$ in the assays resulted in a substantial increase of the catalytic activity of the kinase domain, as noted previously; Mohammadi et al., 1993; Wedegaertner and Gill, 1989). The substrate peptide was derived from the region spanning Y1173 in EGFR (TAENAEYLRVAPQ). All the proteins used in this assay contain the N-terminal $(His)_6$ tag unless otherwise noted. The protein concentrations of the EGFR kinase domain used in the assay range from 3.5 to 14 μM. The total concentration of the DOGS-NTA-Ni in the bulk solution was kept at 12.5 μM in all the assays with DOGS-NTA-Ni-containing vesicles. For assays of the kinase domain attached to vesicles, the protein and vesicles were preincubated at 4°C for ~5 min.

The wild-type EGFR kinase domain was mixed with vesicles containing 0, 0.5, 1, 2, and 5 mole percent of DOGS-NTA-Ni prior to the start of the assay. The final concentration of the protein in the assay was 3.5 μM. The substrate peptide concentration used in these assays was 1 mM. A sample of the kinase domain in the absence of lipid vesicles was also assayed using the same setup as a control.

For comparing the specific activity of the wild-type and various mutant forms of the EGFR kinase domain in the presence and absence of lipid vesicles, the density of DOGS-NTA-Ni on lipid vesicles was kept at 5 mole percent. Preliminary experiments using the substrate peptide at various concentrations showed that the value of K_M for the wild-type kinase domain and this substrate peptide was greater than 4 mM. Due to this high value of K_M, the values of K_M and k_{cat} were not measured directly. Instead, the value of k_{cat}/K_M was derived from a linear fit to the data obtained, using concentrations of the peptide that are much lower than the estimated value of K_M ($V = [S]V_{max}/(K_M + [S])$, $V \approx (V_{max}/K_M)[S]$ when $[S] << K_M$, $k_{cat} = V_{max}$/amount of the enzyme, where V and V_{max} are the initial velocity and maximum initial velocity, respectively). A detailed description of reaction conditions is given in Table S2.

Crystallization and Structure Determination

The two ATP analog-peptide conjugates used for cocrystallization with the kinase domain were synthesized as described (Parang et al., 2001). The peptide sequences are AEEEIYGEFEAKK (the Src substrate peptide; Levinson et al., 2006) and ENAEYLRVAPQK (from a region that spans Tyr1173 in EGFR). The wild-type kinase domain with the His-tag removed (containing an N-terminal tri-peptide with sequence "GAM" from the vector and residues 682–998 from EGFR) at 6 mg/ml was used for the crystallization trials. The V924R mutant in complex with AMP-PNP was crystallized at 8 mg/ml. Crystallization conditions and structural refinement statistics are summarized in Table S3.

Mammalian Cell-Based Signaling Analysis

The EGFR full-length gene with a fragment encoding an N-terminal FLAG antibody recognition sequence (DYKDDDDK) inserted between the 24-residue signal peptide and the mature protein was amplified by PCR and cloned into the pcDNA3.1 vector (BD Biosciences) using XhoI and XbaI restriction enzymes. Mutations were generated by using the Quikchange site-directed mutagenesis kit. All the plasmids used for transfection were prepared using the HiSpeed Plasmid Midi kit (Qiagen) and the sequences were confirmed by DNA sequencing before use.

NIH3T3 cells (which express low levels of endogenous EGFR that are undetectable by Western blot; Bishayee et al., 1999) were cultured in Dulbecco's modified Eagle's medium supplemented with 10% fetal bovine serum, streptomycin/penicillin, sodium pyruvate, and nonessential amino acids (all from Gibco) at 37°C with 5% CO_2. Cells were plated and cultured overnight in 6-well plates in the same medium without antibiotics for transfection. Cells were transfected using Fugene 6 (Roche) according to the manufacturer's instructions with a DNA:Fugene 6 ratio of 1.5 μg:4.5 μl when cells reached ~50% confluency. Cells were cultured for ~36 hr after transfection and serum-starved for ~12 hr before ligand stimulation and harvesting. Ligand stimulation of cells was performed using 50 ng/ml EGF (PeproTech, Inc) at 37°C for 5 min. Cells were lysed in a buffer containing 50 mM Tris, 150 mM NaCl, 1 mM EDTA, 1 mM Na_3VO_4, 1 mM NaF, 1% Triton X-100, and a protease inhibitor cocktail (Roche), pH 7.5. The lysates were centrifuged at 14000 × g for 10 min to remove insoluble material. The supernatants were collected and the protein concentrations were determined using the Bradford protein assay (Bio-Rad) for normalizing the total amount of proteins loaded onto the gels. Samples were run on SDS gels and subjected to Western blot analysis. The total amount of EGFR was monitored using an anti-FLAG antibody (Sigma). The levels of phosphorylation of EGFR at three sites were monitored using anti-EGFR antibodies specific for phosphorylation at Tyr1045 (Cell Signaling), Tyr1068 (Cell signaling), and Tyr1173 (Santa Cruz) (See Supplemental Data for details).

Supplemental Data

Supplemental Data include six figures, three tables, and supplemental text and can be found with this article online at http://www.cell.com/cgi/content/full/125/6/1137/DC1/.

ACKNOWLEDGMENTS

We thank Xiaoxian Cao and Ann Fisher for support of cell culture; David King for mass spectrometry and peptide synthesis; Nick Levinson, Patricia Pellicena, and Lore Leighton for technical help. We also thank Tom Alber, Dafna Bar-Sagi, Rashna Bhandari, Wendy Fantl, Jay Groves, Chafen Lu, G. Steven Martin, Holger Sondermann, Tim Springer, Dane Wittrup, and members of the Kuriyan laboratory for helpful discussions. This work is supported in part by grants from the NIC to P.A.C. (RO1 CA74305) and J.K. (RO1 CA96504).

Received: March 27, 2006
Revised: April 24, 2006
Accepted: May 2, 2006
Published: June 15, 2006

REFERENCES

Barker, S.C., Kassel, D.B., Weigl, D., Huang, X., Luther, M.A., and Knight, W.B. (1995). Characterization of pp60c-src tyrosine kinase activities using a continuous assay: autoactivation of the enzyme is an

intermolecular autophosphorylation process. Biochemistry *34*, 14843–14851.

Bishayee, A., Beguinot, L., and Bishayee, S. (1999). Phosphorylation of tyrosine *992*, 1068, and 1086 is required for conformational change of the human epidermal growth factor receptor C-terminal tail. Mol. Biol. Cell *10*, 525–536.

Burgess, A.W., Cho, H.S., Eigenbrot, C., Ferguson, K.M., Garrett, T.P., Leahy, D.J., Lemmon, M.A., Sliwkowski, M.X., Ward, C.W., and Yokoyama, S. (2003). An open-and-shut case? Recent insights into the activation of EGF/ErbB receptors. Mol. Cell *12*, 541–552.

Burke, C.L., and Stern, D.F. (1998). Activation of Neu (ErbB-2) mediated by disulfide bond-induced dimerization reveals a receptor tyrosine kinase dimer interface. Mol. Cell. Biol. *18*, 5371–5379.

Chang, C.M., Shu, H.K., Ravi, L., Pelley, R.J., Shu, H., and Kung, H.J. (1995). A minor tyrosine phosphorylation site located within the CAIN domain plays a critical role in regulating tissue-specific transformation by erbB kinase. J. Virol. *69*, 1172–1180.

Cho, H.S., and Leahy, D.J. (2002). Structure of the extracellular region of HER3 reveals an interdomain tether. Science *297*, 1330–1333.

De Bondt, H.L., Rosenblatt, J., Jancarik, J., Jones, H.D., Morgan, D.O., and Kim, S.H. (1993). Crystal structure of cyclin-dependent kinase 2. Nature *363*, 595–602.

Deb, T.B., Su, L., Wong, L., Bonvini, E., Wells, A., David, M., and Johnson, G.R. (2001). Epidermal growth factor (EGF) receptor kinase-independent signaling by EGF. J. Biol. Chem. *276*, 15554–15560.

Dorn, I.T., Neumaier, K.R., and Tampe, R. (1998). Molecular recognition of histidine-tagged molecules by metal-chelating lipids monitored by fluorescence energy transfer and correlation spectroscopy. J. Am. Chem. Soc. *120*, 2753–2763.

Ferguson, K.M., Berger, M.B., Mendrola, J.M., Cho, H.S., Leahy, D.J., and Lemmon, M.A. (2003). EGF activates its receptor by removing interactions that autoinhibit ectodomain dimerization. Mol. Cell *11*, 507–517.

Garrett, T.P., McKern, N.M., Lou, M., Elleman, T.C., Adams, T.E., Lovrecz, G.O., Zhu, H.J., Walker, F., Frenkel, M.J., Hoyne, P.A., et al. (2002). Crystal structure of a truncated epidermal growth factor receptor extracellular domain bound to transforming growth factor alpha. Cell *110*, 763–773.

Gotoh, N., Tojo, A., Hino, M., Yazaki, Y., and Shibuya, M. (1992). A highly conserved tyrosine residue at codon 845 within the kinase domain is not required for the transforming activity of human epidermal growth factor receptor. Biochem. Biophys. Res. Commun. *186*, 768–774.

Groenen, L.C., Walker, F., Burgess, A.W., and Treutlein, H.R. (1997). A model for the activation of the epidermal growth factor receptor kinase: involvement of an asymmetric dimer? Biochemistry *36*, 3826–3836.

Huse, M., and Kuriyan, J. (2002). The conformational plasticity of protein kinases. Cell *109*, 275–282.

Jeffrey, P.D., Russo, A.A., Polyak, K., Gibbs, E., Hurwitz, J., Massague, J., and Pavletich, N.P. (1995). Mechanism of CDK activation revealed by the structure of a cyclinA-CDK2 complex. Nature *376*, 313–320.

Jiang, J., Greulich, H., Janne, P.A., Sellers, W.R., Meyerson, M., and Griffin, J.D. (2005). Epidermal growth factor-independent transformation of Ba/F3 cells with cancer-derived epidermal growth factor receptor mutants induces gefitinib-sensitive cell cycle progression. Cancer Res. *65*, 8968–8974.

Kashles, O., Yarden, Y., Fischer, R., Ullrich, A., and Schlessinger, J. (1991). A dominant negative mutation suppresses the function of normal epidermal growth factor receptors by heterodimerization. Mol. Cell. Biol. *11*, 1454–1463.

Landau, M., Fleishman, S.J., and Ben-Tal, N. (2004). A putative mechanism for downregulation of the catalytic activity of the EGF receptor via direct contact between its kinase and C-terminal domains. Structure (Camb.) *12*, 2265–2275.

Levinson, N.M., Kuchment, O., Shen, K., Young, M.A., Koldobskiy, M., Karplus, M., Cole, P.A., and Kuriyan, J. (2006). A Src-like inactive conformation in the Abl tyrosine kinase domain. PLoS Biol. *4*, e144 10.1371/journal.pbio.0040144.

Lynch, T.J., Bell, D.W., Sordella, R., Gurubhagavatula, S., Okimoto, R.A., Brannigan, B.W., Harris, P.L., Haserlat, S.M., Supko, J.G., Haluska, F.G., et al. (2004). Activating mutations in the epidermal growth factor receptor underlying responsiveness of non-small-cell lung cancer to gefitinib. N. Engl. J. Med. *350*, 2129–2139.

McLaughlin, S., Smith, S.O., Hayman, M.J., and Murray, D. (2005). An electrostatic engine model for autoinhibition and activation of the epidermal growth factor receptor (EGFR/ErbB) family. J. Gen. Physiol. *126*, 41–53.

Mohammadi, M., Honegger, A., Sorokin, A., Ullrich, A., Schlessinger, J., and Hurwitz, D.R. (1993). Aggregation-induced activation of the epidermal growth factor receptor protein tyrosine kinase. Biochemistry *32*, 8742–8748.

Moriki, T., Maruyama, H., and Maruyama, I.N. (2001). Activation of preformed EGF receptor dimers by ligand-induced rotation of the transmembrane domain. J. Mol. Biol. *311*, 1011–1026.

Ogiso, H., Ishitani, R., Nureki, O., Fukai, S., Yamanaka, M., Kim, J.H., Saito, K., Sakamoto, A., Inoue, M., Shirouzu, M., and Yokoyama, S. (2002). Crystal structure of the complex of human epidermal growth factor and receptor extracellular domains. Cell *110*, 775–787.

Paez, J.G., Janne, P.A., Lee, J.C., Tracy, S., Greulich, H., Gabriel, S., Herman, P., Kaye, F.J., Lindeman, N., Boggon, T.J., et al. (2004). EGFR mutations in lung cancer: correlation with clinical response to gefitinib therapy. Science *304*, 1497–1500.

Pao, W., Miller, V., Zakowski, M., Doherty, J., Politi, K., Sarkaria, I., Singh, B., Heelan, R., Rusch, V., Fulton, L., et al. (2004). EGF receptor gene mutations are common in lung cancers from "never smokers" and are associated with sensitivity of tumors to gefitinib and erlotinib. Proc. Natl. Acad. Sci. USA *101*, 13306–13311.

Parang, K., Till, J.H., Ablooglu, A.J., Kohanski, R.A., Hubbard, S.R., and Cole, P.A. (2001). Mechanism-based design of a protein kinase inhibitor. Nat. Struct. Biol. *8*, 37–41.

Schindler, T., Sicheri, F., Pico, A., Gazit, A., Levitzki, A., and Kuriyan, J. (1999). Crystal structure of Hck in complex with a Src family-selective tyrosine kinase inhibitor. Mol. Cell *3*, 639–648.

Schlessinger, J. (2002). Ligand-induced, receptor-mediated dimerization and activation of EGF receptor. Cell *110*, 669–672.

Schreiber, A.B., Libermann, T.A., Lax, I., Yarden, Y., and Schlessinger, J. (1983). Biological role of epidermal growth factor-receptor clustering. Investigation with monoclonal anti-receptor antibodies. J. Biol. Chem. *258*, 846–853.

Shigematsu, H., and Gazdar, A.F. (2006). Somatic mutations of epidermal growth factor receptor signaling pathway in lung cancers. Int. J. Cancer *118*, 257–262.

Shigematsu, H., Lin, L., Takahashi, T., Nomura, M., Suzuki, M., Wistuba, I.I., Fong, K.M., Lee, H., Toyooka, S., Shimizu, N., et al. (2005). Clinical and biological features associated with epidermal growth factor receptor gene mutations in lung cancers. J. Natl. Cancer Inst. *97*, 339–346.

Shrout, A.L., Montefusco, D.J., and Weis, R.M. (2003). Template-directed assembly of receptor signaling complexes. Biochemistry *42*, 13379–13385.

Sordella, R., Bell, D.W., Haber, D.A., and Settleman, J. (2004). Gefitinib-sensitizing EGFR mutations in lung cancer activate anti-apoptotic pathways. Science *305*, 1163–1167.

Stamos, J., Sliwkowski, M.X., and Eigenbrot, C. (2002). Structure of the epidermal growth factor receptor kinase domain alone and in

complex with a 4-anilinoquinazoline inhibitor. J. Biol. Chem. *277*, 46265–46272.

Ushiro, H., and Cohen, S. (1980). Identification of phosphotyrosine as a product of epidermal growth factor-activated protein kinase in A-431 cell membranes. J. Biol. Chem. *255*, 8363–8365.

Wedegaertner, P., and Gill, G. (1989). Activation of the purified protein tyrosine kinase domain of the epidermal growth factor receptor. J. Biol. Chem. *264*, 11346–11353.

Wood, E.R., Truesdale, A.T., McDonald, O.B., Yuan, D., Hassell, A., Dickerson, S.H., Ellis, B., Pennisi, C., Horne, E., Lackey, K., et al. (2004). A unique structure for epidermal growth factor receptor bound to GW572016 (Lapatinib): relationships among protein conformation, inhibitor off-rate, and receptor activity in tumor cells. Cancer Res. *64*, 6652–6659.

Xu, W., Doshi, A., Lei, M., Eck, M.J., and Harrison, S.C. (1999). Crystal structures of c-Src reveal features of its autoinhibitory mechanism. Mol. Cell *3*, 629–638.

Yarden, Y., and Schlessinger, J. (1987). Self-phosphorylation of epidermal growth factor receptor: evidence for a model of intermolecular allosteric activation. Biochemistry *26*, 1434–1442.

Yarden, Y., and Sliwkowski, M.X. (2001). Untangling the ErbB signalling network. Nat. Rev. Mol. Cell Biol. *2*, 127–137.

Accession Numbers

The coordinates for structures solved in this study were deposited in the Protein Data Bank with ID codes 2GS2, 2GS6, and 2GS7.